Int. J. Solids Structures, 1974, Vol. 10, pp. 735–754. Pergamon Press. Printed in Gt. Britain.

ON SHEAR LAG EFFECTS IN ORTHOTROPIC COMPOSITE BEAMS

A. O. ADEKOLA†
Civil Engineering Department, University of Lagos, Nigeria

(*Received* 28 *June* 1973; *revised* 27 *November* 1973)

Abstract—Based upon the linearised theories of the bending and stretching of thin plates, an analysis is presented for the interaction between non-prismatic beams and an orthotropic concrete plate. It is shown that an exponential representation for the steel beam profiles provides a suitable basis for studying interaction in continuous non-prismatic beams, and for deducing suitable effective widths of slab for design purposes. The influence of "elastic" shear connection modulus is studied, as well as the effect of the varying flexural rigidity of the steel beams. The dependence of interaction on shear connection modulus in continuous beams is demonstrated through deflexion and slip characteristics, and so also is the dependence of interaction on the severity of the variation of flexural rigidity. The solution can be specialised to the limiting case of prismatic steel beams and a concrete slab and also to the solutions of rectangular plates with certain edge conditions.

INTRODUCTION

Earlier works on shear lag in composite beams [1–4], and others have been limited to thin concrete plates, assumed isotropic, acting compositely with simply supported steel or reinforced concrete ribs, and have not taken into account the influence of the interface elastic shear connection (in the form of studs or dowels) on shear lag. Mention must also be made of an earlier paper by Newmark *et al.* [5] on the influence of shear connectors in composite beams which, however, ignored interface uplift. A more comprehensive investigation which took this into consideration was later presented by Adekola [6], while another recent paper by Adekola [7] investigated the influence of elastic shear connection (in the form of studs or dowels) on shear lag in the concrete plate of interacting prismatic beams and an "isotropic" concrete plate. One significant conclusion of [7] is that effective widths based on deflexion considerations are more rational than those based on concrete plate in-plane membrane stress considerations.

The first part of this paper deals with the interaction of steel ribs elastically connected by means of shear connectors to an orthotropic plate. The results are suitable for studying situations where, in addition to longitudinal ribs, lateral or secondary ribs, either of reinforced concrete or steel beams, exist. The present work not only incorporates the influence of the elastic shear connection, but also extends the theory to continuous beams with an exponential profile, as a convenient idealisation of the more common typical non-prismatic profiles of continuous bridges.

Making use of Hubers [8] elastic constants for a concrete plate, the second part of the analysis deals extensively with the case of equal real roots of the characteristic equations.

† Professor of Civil Engineering.

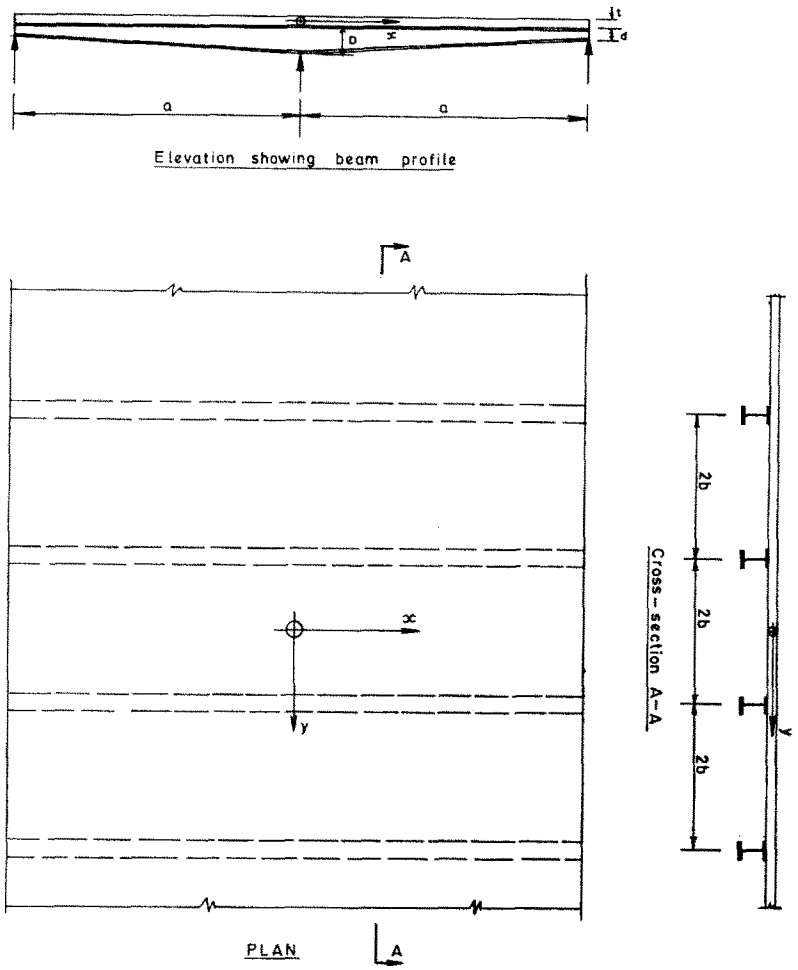

Fig. 1. Coordinate system, beam profile and, composite assembly crosssection.

This is motivated by the fact that concrete is the material commonly used for bridge decks. Of course, the results obtained are easily specialised to the case of complete isotropy.

The results reveal the marked effect of shear connection modulus, k_s, as well as the influence of the severity of flexural rigidity variation $\left(\text{represented by } \frac{d}{D}\right)$ on transverse deflexion. The slip also exhibits a characteristic that does not appear to have been previously noticed. Effective width of a slab acting with a steel beam has been deduced by taking the external moment as an invariant and, thereby, using the moment–curvature relationship to deduce a new increased stiffness at any point over that for the steel beam alone at that point. Effective widths so determined show that as the shear connection modulus, k_s, increases effective width values increase correspondingly, thereby resulting in increased flexural rigidity of the composite assembly. All these are shown in the form of graphs and tables.

A uniformity of method has been maintained by employing potential functions for both the displacement and stresses, as well as the deflexion surface, using Fourier series representation.

FORMULATION OF THE PROBLEM

We are concerned here with the transverse and lateral deformations of an orthotropic elastic plate occupying the region $|x| < a$, $|y| < \infty$, where (x, y) denotes the two-dimensional rectangular cartesian co-ordinates.

In the absence of body forces, the fundamental system of field equations which govern the equilibrium problem for orthotropic plates is:

The stress-displacement equations

$$\left.\begin{aligned} \sigma_{xx} &= c_{11}\frac{\partial U_x}{\partial x} + c_{12}\frac{\partial U_y}{\partial y} \\ \sigma_{yy} &= c_{12}\frac{\partial U_x}{\partial x} + c_{22}\frac{\partial U_y}{\partial y} \\ \sigma_{xy} &= c_{66}\left(\frac{\partial U_x}{\partial y} + \frac{\partial U_y}{\partial x}\right) \end{aligned}\right\} \tag{1}$$

The displacement equilibrium equations

$$\left.\begin{aligned} c_{11}\frac{\partial^2 U_x}{\partial x^2} + (c_{12} + c_{66})\frac{\partial^2 U_y}{\partial x\,\partial y} + c_{66}\frac{\partial^2 U_x}{\partial y^2} &= 0 \\ c_{22}\frac{\partial^2 U_y}{\partial y^2} + (c_{12}\,c_{66})\frac{\partial^2 U_x}{\partial x\,\partial y} + c_{66}\frac{\partial^2 U_y}{\partial x^2} &= 0 \end{aligned}\right\} \tag{2}$$

where c_{ij}'s are elastic constants. With straightforward algebraic manipulations a general solution of the preceeding equations is:

$$\left.\begin{aligned} U_x &= \frac{\partial}{\partial x}(\Psi_1 + \Psi_2) \\ U_y &= \frac{\partial}{\partial y}(\beta_1\Psi_1 + \beta_2\Psi_2) \\ \sigma_{xx} &= c_{11}\frac{\partial^2}{\partial x^2}(\Psi_1 + \Psi_2) + c_{12}\frac{\partial^2}{\partial y^2}(\beta_1\Psi_1 + \beta_2\Psi_2) \\ \sigma_{yy} &= c_{12}\frac{\partial^2}{\partial x^2}(\Psi_1 + \Psi_2) + c_{22}\frac{\partial^2}{\partial y^2}(\beta_1\Psi_1 + \beta_2\Psi_2) \\ \sigma_{xy} &= c_{66}\frac{\partial^2}{\partial x\,\partial y}(\Psi_1 + \Psi_2 + \beta_1\Psi_1 + \beta_2\Psi_2) \end{aligned}\right\} \tag{3}$$

where α_i and β_i are constants connected through

$$\left.\begin{aligned} \alpha_i^2 &= [(c_{12} + c_{66})\beta_i + c_{66}]c_{11}^{-1} \\ &= [c_{12} + c_{66}(1 + \beta_i)]^{-1}c_{22}\beta_i \end{aligned}\right\} \tag{4}$$

from which we deduce that the constants α_i are the roots of the equation:

$$c_{11}c_{66}\alpha^4 + [(c_{12}+c_{66})^2 - c_{66}^2 - c_{11}c_{22}]\alpha^2 + c_{22}c_{66} = 0. \tag{5}$$

The satisfaction of the equilibrium equations shows that the functions Ψ_i satisfy the equations

$$\left(\frac{\partial^2}{\partial x^2} + \alpha_i^2 \frac{\partial^2}{\partial y^2}\right)\Psi_i = 0, \qquad i = 1, 2. \tag{6}$$

In the case of equal real roots it can easily be shown that the complete solution of the field equations becomes

$$\left.\begin{aligned}
U_x &= \frac{\partial \psi}{\partial x} - 4(1+\nu)^{-1}\chi \\
\alpha U_y &= \frac{\partial \psi}{\partial Y} - 4(1+\nu)^{-1}\chi \\
\frac{\sigma_{xx}}{c_{11}} &= \left(\frac{\partial^2}{\partial x^2} + \nu\frac{\partial^2}{\partial Y^2}\right)\psi - 4(1+\nu)^{-1}\left(\frac{\partial \chi}{\partial x} + \nu\frac{\partial \Psi}{\partial Y}\right) \\
\frac{\sigma_{yy}}{\alpha^2 c_{11}} &= \left(\nu\frac{\partial^2}{\partial x^2} + \frac{\partial^2}{\partial Y^2}\right)\psi - 4(1+\nu)^{-1}\left(\nu\frac{\partial \chi}{\partial x} + \frac{\partial \Psi}{\partial Y}\right) \\
\frac{\sigma_{xy}}{\alpha^2 c_{11}} &= (1-\nu)\left\{\frac{\partial^2 \psi}{\partial x\,\partial Y} - 2(1+\nu)^{-1}\left(\frac{\partial}{\partial x} + \frac{\partial}{\partial Y}\right)\chi\right\}
\end{aligned}\right\} \tag{7}$$

where

$$\psi = \phi + x\chi + Y\Psi, \qquad Y = \frac{y}{\alpha}. \tag{8}$$

Equations (7) are analogous to the Papkovich–Neuber representation of the solution of the field equations of equilibrium for isotropic bodies.

On the other hand, the field equations associated with the bending and transverse deflexion of an orthotropic plate are given by

$$\left.\begin{aligned}
M_x &= -\left\{D_x\frac{\partial^2 w}{\partial x^2} + D_1\frac{\partial^2 w}{\partial y^2}\right\}, \\
M_y &= -\left\{D_y\frac{\partial^2 w}{\partial y^2} + D_1\frac{\partial^2 w}{\partial x^2}\right\} \\
M_{xy} &= 2D_{xy}\frac{\partial^2 w}{\partial x\,\partial y},
\end{aligned}\right\} \tag{9}$$

$$D_x\frac{\partial^4 w}{\partial x^4} + 2H\frac{\partial^4 w}{\partial x^2 \partial y^2} + D_y\frac{\partial^4 w}{\partial y^4} = q, \tag{10}$$

where w stands for the deflexion, M_x and M_y for the bending moments and M_{xy} for the torsional moment, q for the load, and H, D_x, D_y, D_1, D_{xy} for constants characterising the rigidity of the plate.

To the foregoing equations are to be adjoined the conditions of simply supported edges; namely

$$w = M_x = 0 \tag{11}$$

for $x = \pm a$, $y = \pm(2n-1)b$, $n = 1, 2$, etc.;
the conditions of stress free edges: namely

$$\sigma_{xx} = \sigma_{xy} = 0 \tag{12}$$

for $x = \pm a$, $|y| < \infty$;
the conditions of symmetry

$$U_y = \frac{\partial w}{\partial y} = 0 \tag{13}$$

for $|x| < a$, $y = 0$;
and the condition of equilibrium of internal and external forces and moments at the cross-section of each longitudinal rib.

$$\frac{\partial^2 M_r}{\partial x^2} + \frac{1}{2}\frac{\partial}{\partial x}\left(d_x \frac{\partial F}{\partial x}\right) - \frac{\partial Q_c}{\partial x} + p' = 0 \tag{14}$$

where

$$Q_{c,1} = -2\frac{\partial}{\partial y}\left\{D_y \frac{\partial^2 w}{\partial y^2} + H\frac{\partial^2 w}{\partial x^2}\right\}, \tag{15}$$

and the overall depth of the non-prismatic beam d_x at any section x is given by

$$d_x = De^{-\varepsilon|x|}. \tag{16}$$

The corresponding second moment of area $I(x)$ for a symmetrical I-shaped cross-section having the profile of 16 is representable by

$$I(x) = I_0 \sum_{r=0}^{3} J_r e^{-r\varepsilon|x|} \tag{17}$$

where J_r's are non-dimensional constants characterising the geometry of the section, and ε is another constant.

$$\frac{\partial^2 M_r}{\partial x^2} = -E_s\{I(x) \cdot w_{,1111} + 2I(x)_{,1} \cdot w_{,111} + I(x)_{,11} \cdot w_{,11}\}. \tag{18}$$

where $(x, y) = (x_1, x_2)$ represents the two-dimensional coordinates while a comma followed by an index implies partial differentiation with respect to the corresponding variable.

$$\frac{\partial F}{\partial x} = -t\int_{-b}^{b} \frac{\partial \sigma_{xx}}{\partial x}\,dy, \tag{19}$$

which implies that

$$F = 2t\,c_{66} \sum_{i=1}^{2} (1 + \beta_i) \frac{\partial \Psi_i}{\partial y}\bigg|_{y=b}.$$

Finally, we must satisfy the following condition of compatibility of longitudinal strains at the slab-beam junctions in the following manner (see for example [7] for the arguments leading to the derivation of this relation):

$$(ER)^{-1}F + \tfrac{1}{2}(d_x + t)w_{,11} - \frac{\partial U_x}{\partial x} = k_s^{-1}F_{,11}, \tag{20}$$

where k_s is the modulus of shear connection, whilst the cross-sectional area of the steel I-section, R, at any point x is of the form

$$R = R_0(k_0 + k_1 e^{-\varepsilon|x|}) \tag{21}$$

R_0 being the cross-sectional area at the origin, and the constants characterising the geometry of the section are k_0 and k_1.

We must also satisfy the conditions of symmetry in the lateral direction (i.e. y direction)

$$U_y = \frac{\partial w}{\partial y} = 0$$

$$\text{at } y = \pm(2n-1)b, \ |x| < a. \tag{22}$$

METHOD OF SOLUTION

Assuming that the load q admits of the Fourier series representations

$$q = D_x \sum_{n=1}^{\infty} q_n \cos(K_n x), \tag{23}$$

we construct the deflexion surface in the form

$$w(x, y) = \sum_{n=1}^{\infty} \left\{ K_n^{-4} q_n + \sum_{i=1}^{2} A_{ni}^* \cosh(K_n Y_i) \right\} \cos(K_n x) \tag{24}$$

for distinct real roots, and

$$w(x, y) = \sum_{n=1}^{\infty} \{ K_n^{-} q_n + \bar{A}_{n_1}^* \cosh(K_n Y) + \bar{A}_{n_2}^* Y \sinh(K_n Y) \} \cos(K_n x) \tag{25}$$

for equal real roots, where $A_{n_1}^*$, $A_{n_2}^*$, $\bar{A}_{n_1}^*$ and $\bar{A}_{n_2}^*$ are as yet undetermined superposition coefficient, while

$$\lambda_i^2 = \frac{H}{D_x} \pm \sqrt{\left(\frac{H}{D_x}\right)^2 - \frac{D_y}{D_x}}, \qquad H = D_1 + 2D_{xy}$$

$$Y_i = y/\lambda_i \qquad i = 1, 2$$

and assuming Huber's elastic constants† for concrete

$$D_1 = \nu\sqrt{D_x D_y}, \qquad D_{xy} = \frac{1-\nu}{2}\sqrt{D_x D_y} \quad \text{and} \quad H = \sqrt{D_x D_y}$$

we obtain the case of equal real roots with

$$\lambda = \sqrt[4]{\frac{D_y}{D_x}}$$

$$Y = y/\lambda.$$

Now and henceforth a bar $(-)$ on any superposition coefficient would refer to the case of equal real roots.

† From these constants, the relationship between the constants c_{11}, c_{22}, c_{12}, and c_{66} can be deduced for concrete.

We now construct the stress functions suited for the solution of our problem as follows: For distinct real roots,

$$\Psi(x, y) = \sum_{n=1}^{\infty} \{A_{nm} \cosh(K_n y_m)\cos(K_n x) + B_{nm} \cos(L_n y)\cosh(L_n x_m)\}. \tag{26}$$

For equal real roots,

$$\left.\begin{aligned} \phi &= \sum_{n=1}^{\infty} (\bar{A}_{n_1} \cosh(K_n Y)\cos(K_n x) + \bar{B}_n \cosh(L_n X)\cos(L_n y)) \\ \Psi &= \sum_{n=1}^{\infty} \bar{A}_{n_1} \sinh(K_n Y)\cos(K_n x) \\ \chi &= \sum_{n=1}^{\infty} \bar{B}_{n_2} \sinh(L_n X)\cos(L_n y) \end{aligned}\right\} \tag{27}$$

where A_{n_1}, A_{n_2}, $\bar{A}_{n_1}$, $\bar{A}_{n_2}$, B_{n_1}, B_{n_2}, $\bar{B}_{n_1}$ and $\bar{B}_{n_2}$ are again undetermined superposition coefficients, Y retains its previous definition whilst

$$X = \alpha x, \qquad y_m = y/\alpha_m, \qquad x_m = \alpha_m x$$
$$m = 1, 2, \qquad K_n = (2n-1)\pi/2a, \qquad L_n = (2n-1)\pi/b.$$

By applying the boundary conditions of (12), (13) and (22), and by employing certain routine mathematical techniques ([9], p. 198, 2·671) we obtain relationships between the various superposition coefficients for the deflexion surface and the stress functions respectively. These techniques are omitted in this paper, however these relations are simply stated here as follows:

$$A^*_{n_1} = \frac{\lambda_1 \sinh(K_n b\lambda_2^{-1})}{\lambda_2 \sinh(K_n b\lambda^{-1})} A^*_{n_2} \tag{28}$$

$$\bar{A}^*_{n_1} = -K_n^{-1}\{1 + K_n b\lambda^{-1} \coth(K_n b\lambda^{-1})\}\bar{A}^*_{n_2} \tag{29}$$

$$A_{n_1} = -\frac{\alpha_1 \beta_2 \sinh(K_n b\alpha_2^{-1})}{\alpha_2 \beta_1 \sinh(K_n b\alpha_1^{-1})} A_{n_2} \tag{30}$$

$$\bar{A}_{n_1} = K_n^{-1}\left\{\frac{3-\nu}{1+\nu} - K_n b\alpha^{-1} \coth(K_n b\alpha^{-1})\right\}\bar{A}_{n_2} \tag{31}$$

$$B_{n_1} = -\frac{(1+\beta_2)\cosh(L_n \alpha_2 a)}{(1+\beta_1)\cosh(L_n \alpha_1 a)} B_{n_2} \tag{32}$$

$$\bar{B}_{n_1} = L_n^{-1}(\alpha^2 c_{11} - c_{12})^{-1}\left\{\frac{2(1-\nu)c_{11}}{1+\nu} - (\alpha^2 c_{11} - c_{12})L_n a \tanh(L_n a)\right\}\bar{B}_{n_2} \tag{33}$$

$$B_r = 2L_r \sum_{i=1}^{2} (1+\beta_i)(\alpha_i b)^{-1} \sum_{m=1}^{\infty} \frac{(-1)^m K_m^2 \sinh(K_m b\alpha_i^{-1})}{[L_r^2 + \alpha_i^{-2} K_m^2]} A_{mi}, \tag{34}$$

$$\bar{B}_r = 4b^{-1} \sum_{m=1}^{\infty} \frac{(-1)^m L_r K_m \alpha^{-1} \sinh(K_m b\alpha^{-1})}{\alpha^{-2} K_m^2 + L_r^2} \left\{(1+\nu)^{-1} - \frac{\alpha^{-2} K_m^2}{\alpha^{-2} K_m^2 + L_r^2}\right\}\bar{A}_{m_2} \tag{35}$$

where

$$B_r = (1+\beta_2)L_r^2 \cosh(L_r\alpha_2 a)\{\alpha_2 \tanh(L_r\alpha_2 a) - \alpha_1 \tanh(L_r\alpha_1 a)\}B_{r_2}, \tag{36}$$

$$\bar{B}_r = L_r\left\{\frac{(1-\nu)(\alpha^2 c_{11}+c_{12})}{(1+\nu)(\alpha^2 c_{11}-c_{12})}\sinh(L_r\alpha a) + \frac{L_r\alpha a}{\cosh(L_r\alpha a)}\right\}\bar{B}_{r_2}. \tag{37}$$

We now apply the equilibrium condition (14) and again by employing routine mathematical techniques and standard results ([9], p. 196, 2·663; p. 203, 2·674), the equilibrium equation for the composite assembly reduces to

$$A^*_{m2}\{E_0 I_0 J_0 K_m^2 S^*_m + 2\lambda_2^{-1}(\lambda_2^{-2}-\lambda_1^{-2})D_y K_m^3 \sinh(K_m b\lambda_2^{-1})\} + \frac{EI_0}{a}\sum_{n=1}^{\infty} L_{mn}K_n^{-2}S^*_n A^*_{n_2} - \frac{a\,\delta D}{2}\sum_{n=1}^{\infty} F_{mn}A_{n_2} = -[EI_0 J_0 q_m - p_m] - \frac{EI_0}{a}\sum_{n=1}^{\infty} K_n^{-4}L_{mn}q_n, \tag{38}$$

and

$$\bar{A}^*_{m_2}\{E_0 I_0 J_0 K_m \bar{S}^*_m + 4D_y\lambda^{-3}K_m^2 \sinh(K_m b\lambda^{-1})\} + \frac{EI_0}{a}\sum_{n=1}^{\infty} K_n^{-3}L_{mn}\bar{S}^*_n\bar{A}^*_{n_2} + \frac{\Delta D}{2a}\sum_{n=1}^{\infty} F_{mn}\bar{A}_{n_2} = EI_0 J_0 q_m - p_m + \frac{EI_0}{a}\sum_{n=1}^{\infty} K_n^{-4}L_{mn}q_n, \tag{39}$$

where

$$S^*_r = K_r^2\left\{\cosh(K_r b\lambda_2^{-1}) - \frac{\lambda_1 \sinh(K_r b\lambda_2^{-1})}{\lambda_2 \sinh(K_r b\lambda_1^{-1})}\right\}, \tag{40}$$

$$\bar{S}^*_r = K_r^2\left(\cosh(K_r b\lambda^{-1}) + \frac{K_r b\lambda^{-1}}{\sinh(K_r b\lambda^{-1})}\right) \tag{41}$$

$$L_{mn} = \sum_{r=1}^{3} J_r r\varepsilon K_n^2\left\{\frac{[K_n^2 - 2K_nK_m + r^2\varepsilon^2]}{r^2\varepsilon^2 + (K_n-K_m)^2}[(-1)^{n-m}e^{-r\varepsilon a} - 1] - \frac{[K_n^2 + 2K_nK_m + r^2\varepsilon^2]}{r^2\varepsilon^2 + (K_n+K_m)^2}[(-1)^{n+m}e^{-r\varepsilon a} - 1]\right\} \tag{42}$$

and

$$F_{mn} = \varepsilon K_n K_m \sinh(K_m b\alpha_2^{-1})\left\{\frac{1+(-1)^{n+m}e^{-\varepsilon a}}{\varepsilon^2 + (K_n+K_m)^2} - \frac{1-(-1)^{n+m}e^{-\varepsilon a}}{\varepsilon^2 + (K_n-K_m)^2}\right\}. \tag{43}$$

The quantity P_m, the transverse load per unit length acting on the beam element, includes the external applied loads and, in the case of shored beams, the beam self weight P_{ms} which for the beams being considered in this analysis is given by

$$P_{ms} = \frac{2P_0}{a}\left\{(-1)^{m+1}\frac{k_0}{K_m} + \frac{k_1[\varepsilon + (-1)^{m+1}K_m]}{\varepsilon^2 + K_m^2}\right\} \tag{44}$$

where P_0 is the maximum intensity of the self weight.

Employing precisely the same procedure as that used in the satisfaction of the equilibrium equation (14), the satisfaction of the compatibility condition (20) now reduces to

$$\frac{atk_0}{2} S_m^* A_{m_2}^* + \sum_{n=1}^{\infty} R_n^* A_{n_2}^* - S_m A_{m_2} - k_1 k_s^{-1} \sum_{n=1}^{\infty} g_{mn} R_n A_{n_2} - \sum_{n=1}^{\infty} \sum_{r=1}^{\infty} V_{mn} \bar{V}_{rn} A_{r_2}$$

$$= -\frac{ak_0 t}{2} K_m^{-2} q_m - \frac{1}{2} \sum_{n=1}^{\infty} K_n^{-2} \{(k_0 D + k_1 t) g_{mn} + k_1 D h_{mn}\} q_n, \quad (45)$$

for distinct real roots where S_r^* is as previously defined for distinct real roots and

$$S_r = (ER_0)^{-1} a \left\{ \frac{2tc_{66}(\beta_1 - \beta_2)}{\alpha_2 \beta_1} K_r \sinh(K_r b \alpha_2^{-1})[1 + k_0 k_s^{-1} K_r^2 E R_0] \right.$$

$$\left. + k_0 E R_0 K_r^2 \left\{ \cosh(K_r b \alpha_2^{-1}) - \frac{\alpha_1 \beta_2 \sinh(K_r b \alpha_2^{-1})}{\alpha_2 \beta_1 \sinh(K_r b \alpha_1^{-1})} \right\} \right. \quad (46)$$

$$R_r^* = \tfrac{1}{2}\{(k_0 D + k_1 t) g_{mr} + k_1 D h_{mr}\} . S_r^* \quad (47)$$

$$R_r = K_r^2 \left\{ \delta K_r \sinh(K_r b \alpha_2^{-1}) + k_s \left\{ \cosh(K_r b \alpha_2^{-1}) - \frac{\alpha_1 \beta_2 \sinh(K_r b \alpha_2^{-1})}{\alpha_2 \beta_1 \sinh(K_r b \alpha_1^{-1})} \right\} \right\}, \quad (48)$$

$$\delta = 2tc_{66}(\beta_1 - \beta_2)/\alpha_2 \beta_1, \quad (49)$$

$$U_r^{-1} = b^3 \sinh(L_r \alpha_2 a) \left\{ 1 - \frac{\alpha_1 \tanh(L_r \alpha_2 a)}{\alpha_2 \tanh(L_r \alpha_1 a)} \right\}, \quad (50)$$

$$V_{mn} = 2k_0(-1)^{m+1} K_m U_n \left\{ \frac{1 + \beta_2}{1 + \beta_1} \cdot \frac{\alpha_1^2}{(\alpha_1 L_n)^2 + K_m^2} - \frac{\alpha_2^2}{(\alpha_2 L_n)^2 + K_m^2} \right\} L_n \cosh(L_n \alpha_2 a)$$

$$+ k_1 L_n U_n \left\{ \frac{\alpha_1^2 (1 + \beta_2) \cosh(L_n \alpha_2 a)}{(1 + \beta_1) \cosh(L_n \alpha_1 a)} \left\{ \frac{(\varepsilon + \alpha_1 L_n) + (-1)^{m+1} \cdot K_m e^{-(\varepsilon + \alpha_1 L_n)a}}{(\varepsilon + \alpha_1 L_n)^2 + K_m^2} \right.\right.$$

$$\left.\left. + \frac{(\varepsilon - \alpha_1 L_n) + (-1)^{m+1} \cdot K_m e^{-(\varepsilon - \alpha_1 L_n)a}}{(\varepsilon - \alpha_1 L_n)^2 + K_m^2} \right\} \right.$$

$$\left. - \alpha_2^2 \left\{ \frac{(\varepsilon + \alpha_2 L_n) + (-1)^{m+1} \cdot K_m e^{-(\varepsilon + \alpha_2 L_n)a}}{(\varepsilon + \alpha_2 L_n)^2 + K_m^2} + \frac{(\varepsilon - \alpha_2 L_n) + (-1)^{m+1} \cdot K_m e^{-(\varepsilon - \alpha_2 L_n)a}}{(\varepsilon - \alpha_2 L_n)^2 + K_m^2} \right\} \right\}, \quad (51)$$

$$\bar{V}_{rn} = 2(-1)^r K_r^2 b^2 \alpha_2^2 \sinh(K_r b \alpha_2^{-1}) \left\{ \frac{1}{\alpha_2^{-2} K_r^2 + L_n^2} - \frac{\beta_2 (1 + \beta_1)}{\beta_1 (1 + \beta_2)} \cdot \frac{1}{\alpha_1^{-2} K_r^2 + L_n^2} \right\}, \quad (52)$$

and for equal real roots

$$\frac{atk_0}{2} \bar{S}_m^* \bar{A}_{m_2}^* + \sum_{n=1}^{\infty} \bar{R}_n^* \bar{A}_{n_2}^* + \bar{S}_m \bar{A}_{m_2} + k_1 k_s^{-1} \sum_{n=1}^{\infty} g_{mn} \bar{R}_n \bar{A}_{n_2} + \sum_{n=1}^{\infty} \sum_{r=1}^{\infty} V_{mn} \bar{V}_{rn} \bar{A}_{r_2}$$

$$= \frac{ak_0 t}{2} K_m^{-2} q_m + \frac{1}{2} \sum_{n=1}^{\infty} K_n^{-2} \{(k_0 D + k_1 t) g_{mn} + k_1 D h_{mn}\} q_n, \quad (53)$$

where the constant S_r^* takes the previous corresponding definition and the other constants now take the form

$$\bar{S}_r = a\Delta[(ER_0)^{-1} + k_0 k_s^{-1} k_r^2]\sinh(K_r b\alpha^{-1}) + k_0 K_r a\left\{\frac{3-\nu}{1+\nu}\cosh(K_r b\alpha^{-1}) - \frac{K_r b\alpha^{-1}}{\sinh(K_r b\alpha^{-1})}\right\}, \tag{54}$$

$$\bar{R}_r^* = \frac{K_r^{-1}}{2}\{(k_0 D + k_1 t)g_{mr} + k_1 D h_{mr}\}.\ S_r, \tag{55}$$

$$\bar{R}_r = K_r\left\{\Delta K_r \sinh(K_r b\alpha^{-1}) + k_s\left\{\frac{3-\nu}{1+\nu}\cdot\cosh(K_r b\alpha^{-1}) - \frac{K_r b\alpha^{-1}}{\sinh(K_r b\alpha^{-1})}\right\}\right\} \tag{56}$$

$$\Delta = 8tc_{66}\alpha^{-1}(1+\nu)^{-1}, \tag{57}$$

$$U_r^{-1} = L_r b\left\{\frac{1-\nu}{1+\nu}\cdot\frac{\alpha^2 c_{11} + c_{12}}{\alpha^2 c_{11} - c_{12}}\sinh(L_n\alpha a) + \frac{L_n\alpha a}{\cosh(L_n\alpha a)}\right\}, \tag{58}$$

$$\begin{aligned} V_{mn} = {} & \frac{4\alpha k_0 L_n K_m(-1)^{m+1}\cosh(L_n\alpha a)}{\alpha^2 L_n^2 + K_m^2}\left\{\frac{(1-\nu)c_{12}}{(1+\nu)(\alpha^2 c_{11} - c_{12})} - \frac{\alpha^2 L_n^2}{\alpha^2 L_n^2 + K_m^2}\right\} \\ & + \alpha k_1 L_m\left(\frac{2(1-\nu)c_{12}}{(1+\nu)(\alpha^2 c_{11} - c_{12})} - L_n\alpha a\tanh(L_n\alpha a)\right) \\ & \times\left\{\frac{\varepsilon + \alpha L_n + (-1)^{m+1}K_m e^{-(\varepsilon-\alpha L_n)a}}{(\varepsilon+\alpha L_n)^2 + K_m^2} + \frac{\varepsilon - \alpha L_n + (-1)^{m+1}\cdot K_m e^{-(\varepsilon-\alpha L_n)a}}{(\varepsilon-\alpha L_n)^2 + K_m^2}\right\} \\ & + \frac{k_1\alpha^2 L_n^2}{[(\varepsilon+\alpha L_n)^2 + K_m^2]^2} \\ & \times\{K_m^2 - (\varepsilon+\alpha L_n)^2 - (-1)^{m+1}\cdot K_m(a[K_m^2 + (\varepsilon+\alpha L_n)^2] + 2(\varepsilon+\alpha L_n))e^{-(\varepsilon+\alpha L_n)a}\} \\ & - \frac{k_1\alpha^2 L_n^2}{[(\varepsilon-\alpha L_n)^2 + K_m^2]^2} \\ & \times\{K_m^2 - (\varepsilon-\alpha L_n)^2 - (-1)^{m+1}K_m(a[K_m^2 + (\varepsilon-\alpha L_n)^2] + 2(\varepsilon-\alpha L_n))e^{-(\varepsilon-\alpha L_n)a}\} \end{aligned} \tag{59}$$

$$\bar{V}_{rn} = \frac{4U_n(-1)^r L_n K_r\alpha^{-1}\sinh(K_r b\alpha)}{\alpha^{-2}K_r^2 + L_n^2}\left\{(1+\nu)^{-1} - \frac{\alpha^{-2}K_r^2}{\alpha^{-2}K_r^2 + L_n^2}\right\}, \tag{60}$$

and for both cases of distinct and equal real roots g_{mn} and h_{mn} have the following definitions

$$g_{mn} = \varepsilon\left\{\frac{1+(-1)^{n+m}\cdot e^{-\varepsilon a}}{\varepsilon^2 + (K_n + K_m)^2} + \frac{1-(-1)^{n-m}\cdot e^{-\varepsilon a}}{\varepsilon^2 + (K_n - K_m)^2}\right\}, \tag{61}$$

$$h_{mn} = 2\varepsilon\left\{\frac{1+(-1)^{n+m}\cdot e^{-2\varepsilon a}}{4\varepsilon^2 + (K_n + K_m)^2} + \frac{1-(-1)^{n-m}\cdot e^{-\varepsilon a}}{4\varepsilon^2 + (K_n - K_m)^2}\right\}. \tag{62}$$

The superposition coefficients $A_{r_2}^*$, $\bar{A}_{r_2}^*$, A_{r_2} and $\bar{A}_{r_2}$ become determinable by solving, through a segmentation procedure, the series equations resulting from the application of the composite assembly's equilibrium and compatibility conditions taking as many terms as we please.

MIDDLE SUPPORT REACTION

The longitudinal profile assumed for the steel beam in the foregoing analysis is that typical of a two-span continuous bridge of the beam-deck type. It is therefore necessary to deduce the value of the middle support reaction arising from applied loading. Let $w_Q(0, b)$ be the deflexion at the support section, $x = 0$, due to the applied loading Q (which may consist of self weight, point load and superimposed load) and $W_R(0, b)$ that due to an applied unit load alone at $x = 0$, then by the principle of superposition, if there is to be no vertical displacement at the middle support section, the unknown central reaction R due to the loading Q is given by

$$R = -\frac{w_Q(0, b)}{W_{R=1}(0, b)}. \tag{63}$$

The transverse deflexion $w(x, y)$ at any point in the plate becomes $w_{(Q)}(x, y) + w_{(R)}(x, y)$ thus introducing new superposition coefficients in the transverse deflexion equation and consequently in the stress functions in the form given below:

$$\left.\begin{aligned} A^*_{cni} &= A^{*(Q)}_{ni} + A^{*(R)}_{ni} \\ \bar{A}^*_{cni} &= \bar{A}^{*(Q)}_{ni} + \bar{A}^{*(R)}_{ni} \\ B_{cni} &= B^{(Q)}_{ni} + B^{(R)}_{ni} \\ &\text{etc.} \end{aligned}\right\}. \tag{64}$$

Using these relations these coefficients, deflexion, displacements, and stresses can be computed.

Case of no interaction

We can infer from the preceeding analysis deflexions for the case when the concrete slab is merely resting on the ribs and not physically connected to them. In that case, the interacting axial forces between the two elements (i.e. concrete plate and steel beam) become zero. Consequently all the superposition coefficients A's and $\bar{A}$'s become zero and the strain compatibility condition becomes indeterminate. Under these circumstances the equilibrium condition alone determines uniquely the solution for no interaction condition. The solution for this condition is obtained by setting A's and $\bar{A}$'s to zero in (38), for the case of distinct real roots, and in (39) for the case of equal real roots, thereby making the corresponding deflexion $w(x, y)$ determinable.

Effective width factor may be defined, from a consideration of membrane stress distribution, as a fraction β_{st} of the available width of the orthotropic slab that contributes, at constant maximum longitudinal stress $\sigma_{xx\,\max}$, a force equal to the interacting axial forces F. Hence

$$\beta_{st} = \frac{-F}{2b\sigma_{xx}|_{y=b}} \tag{65}$$

where F is as previously defined in 19.

An alternative approach in the estimation of effective width factor is to employ the moment-curvature relationship for a beam. Let the moment-curvature relationship for a steel beam alone subjected to a given loading system be given by

$$E_s I_s(x) \cdot w_{0,11} = -M \tag{66}$$

where, at the point x, $E_s I_s(x)$ is the flexural rigidity of the steel beam, M the external moment due to applied loading and w_0 the deflexion of the steel beam. Let us now suppose that a composite section consisting of the same steel beam and a concrete plate under the same conditions of support and loading have an equivalent flexural rigidity $E_s I_c(x)$; the moment-curvature relationship for the new assembly now becomes

$$E_s I_c(x) w_{,11} = -M \tag{67}$$

w being the deflexion at x of the composite section whilst M retains its previous definition.

Since in equations (66) and (67) the bending moment M at the point x is an invariant these two equations combine to give

$$E_s I_c(x) \cdot w_{,11} = E_s I_s(x) \cdot w_{0,11} \tag{68}$$

from which $I_c(x)$ is readily determined. Employing transformed section theory, it is now a simple matter to deduce the effective width factor β_M from the relationship:

$$\beta_M^2 + \frac{\beta_M}{2bt^3 c_{11}} \{E_s R_s(x)(3d_x + 6td_x + 4t^2) - 12(E_s I_c(x) - E_s I_s(x)\} - \frac{3E_s R_s(x)}{b^2 t^4 c_{11}} [E_s I_c(x) - E_s I_s(x)] = 0. \tag{69}$$

Effective width factors deduced from either membrane stresses or moment curvature relationship do not present the true picture in the region of the middle support where cracks would tend to develop in concrete. Nonetheless, by taking concrete together with its reinforcement as an orthotropic material, they provide some estimate of effective widths in this region.

SOME SPECIAL RESULTS

Prismatic beam

The solution for the limiting case of a prismatic steel beam interacting with an orthotropic concrete plate can be obtained by setting ε, the constant parameter defining the beam profile, to zero. In the limit as ε tends to zero we find that L_{mn} tends to zero for all values of n whilst g_{mn} and h_{mn} both tend to zero for all values of n not equal to m and to a when n is equal to m. F_{mn} tends to zero for n not equal to m and to $-K_n^2$ a $\sinh(K_n b\alpha_2^{-1})$ for n equal to m, and

$$V_{mn} \to 2(-1)^{m+1}(k_0 + k_1) K_m L_n U_n \cosh(L_n \alpha_2 a) \left\{ \frac{1 + \beta_2}{1 + \beta_1} \frac{\alpha_1^2}{K_m^2 + \alpha_1^2 L_n^2} - \frac{\alpha_2^2}{K_m^2 + \alpha_2^2 L_n^2} \right\}. \tag{70}$$

From this limiting process the compatibility equations will have the factor $(k_0 + k_1)$ which will cancel out in both equations.

The corresponding equations for an isotropic plate are easily deduced from these results.

Plate bending

The solution for an infinitely long orthotropic rectangular plate simply supported along the edges $x = \pm a$ and carrying equally spaced (along y) transverse point loads can be deduced

from these results by setting EIJ_0 to zero. The transverse deflexion becomes

$$w(x,y) = \sum_{n=1}^{\infty} K_n^{-4}\left\{q_n - \frac{K_n\lambda_1^2\lambda_2^2 P_n}{2D_y(\lambda_1^2-\lambda_2^2)}\left[\frac{\lambda_1\cosh(K_n y\lambda_1^{-1})}{\sinh(K_n b\lambda_1^{-1})} - \frac{\lambda_2\cosh(K_n y\lambda_2^{-1})}{\sinh(K_n b\lambda_2^{-1})}\right]\right\}\cos(K_n x). \tag{71a}$$

We obtain the solution for a rectangular plate simply supported on opposite edges ($x = \pm a$) and clamped at the remaining edges ($y = \pm b$) by setting EIJ_0 to ∞. The deflexion $w(x, y)$ and the moment M_y are as follows

$$w(x,y) = \sum_{n=1}^{\infty} K_n^{-4}q_n\left[1 + \frac{K_n\lambda_1\tanh(K_n b\lambda_2^{-1})\cosh(K_n y\lambda_1^{-1})}{\lambda_2\sinh(K_n b\lambda_1^{-1}) - \lambda_1\tanh(K_n b\lambda_2^{-1})}\right.$$
$$\left. - \frac{K_n\lambda_2\sinh(K_n b\lambda_1^{-1})\operatorname{sech}(K_n b\lambda_2^{-1})\cosh(K_n y\lambda_2^{-1})}{\lambda_2\sinh(K_n b\lambda_1^{-1}) - \lambda_1\tanh(K_n b\lambda_2^{-1})}\right]\cos(K_n x) \tag{72a}$$

$$M_y = D_y\sum_{n=1}^{\infty} K_n^{-1}q_n\left\{\frac{\lambda_2\tanh(K_n b\lambda_2^{-1})\cosh(K_n y\lambda_1^{-1}) - \lambda_1\sinh(K_n b\lambda_1^{-1})\operatorname{sech}(K_n b\lambda_2^{-1})\cosh(K_n y\lambda_2^{-1})}{\lambda_1\lambda_2(\lambda_2\sinh(K_n b\lambda_1^{-1}) - \lambda_1\tanh(K_n b\lambda_2^{-1}))}\right\}\cos(K_n x). \tag{73a}$$

The fixed end moments at $y = \pm b$ are given by

$$M_y|_{y=b} = D_y\sum_{n=1}^{\infty}\frac{K_n^{-1}q_n}{\lambda_1\lambda_2}\left\{\frac{\lambda_2\tanh(K_n b\lambda_2^{-1})\cosh(K_n b\lambda_1^{-1}) - \lambda_1\sinh(K_n b\lambda_1^{-1})}{\lambda_2\sinh(K_n b\lambda_1^{-1}) - \lambda_1\tanh(K_n b\lambda_2^{-1})}\right\}\cos(K_n x). \tag{74a}$$

In the case of equal real roots, with $\lambda_1 = \lambda_2 = \lambda$ say, equations (71a–74a) pass over into

$$w(x,y) = \sum_{n=1}^{\infty} K_n^{-2}\left\{K_n^{-2}q_n - \frac{\lambda^3 P_n}{4D_y\sinh(K_n b\lambda^{-1})}\left[K_n^{-1}(1 + K_n b\lambda^{-1}\coth(K_n b\lambda^{-1}))\right.\right.$$
$$\left.\left.\cdot\cosh(K_n y\lambda^{-1}) - \lambda^{-1}y\sinh(K_n y\lambda^{-1})\right]\right\}\cos(K_n x), \tag{71b}$$

$$w(x,y) = \sum_{n=1}^{\infty} K_n^{-4}q_n\left\{1 - \frac{[\tanh(K_n b\lambda^{-1}) + K_n b\lambda^{-1}]\cosh(K_n y\lambda^{-1}) + K_n y\lambda^{-1}\tanh(K_n b\lambda^{-1})\sinh(K_n y\lambda^{-1})}{\sinh(K_n b\lambda^{-1}) + K_n b\lambda^{-1}\operatorname{sech}(K_n b\lambda^{-1})}\right\}\cos(K_n x) \tag{72b}$$

$$M_y = D_y\sum_{n=1}^{\infty} K_n^2\lambda^{-2}\left\{\frac{[\tanh(K_n b\lambda^{-1}) - K_n b\lambda^{-1}]\cosh(K_n y\lambda^{-1}) + K_n\lambda^{-1}\tanh(K_n b\lambda^{-1})\cdot y\sinh(K_n y\lambda^{-1})}{\sinh(K_n b\lambda^{-1}) + K_n b\lambda^{-1}\operatorname{sech}(K_n b\lambda^{-1})}\right\}\cos(K_n x), \tag{73b}$$

$$M_y|_{y=b} = D_y\sum_{n=1}^{\infty} K_n^2\lambda^{-2}q_n\left\{\frac{\sinh(2K_n b\lambda^{-1}) - 2K_n b\lambda^{-1}}{\sinh(2K_n b\lambda^{-1}) + 2K_n b\lambda^{-1}}\right\}\cos(K_n x). \tag{74b}$$

Data used for computation

$I_0 = 1{\cdot}309\,579 \times 10^{-3}\text{m}^4$
$R_0 = 1{\cdot}969\,300 \times 10^{-2}\text{m}^2$
$a_0 = 0{\cdot}587\,407$
$b_0 = 0{\cdot}412\,593$

Maximum intensity of beam = self weight = 1·49 kN/m
Concrete plate thickness = 0·152 m
Half span of continuous beam = 4·0 m
Applied point load in each span = 250 kN
Based on Hubers constants for concrete [8], the following elastic properties are assumed for the concrete plate.

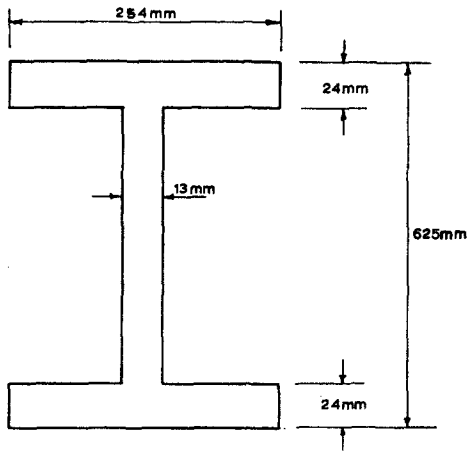

Fig. 2. Dimensions of steel beam at middle support section.

$$D_x = \frac{c_{11}t^3}{12}, \qquad D_Y = \lambda^4 D_x, \qquad H = \lambda^2 D_x$$

$$c_{11} = \frac{E_c}{1-\alpha^4\nu^2}, \; c_{22} = \alpha^4 c_{11}, \; c_{12} = \alpha^2 \nu c_{11},$$

$$c_{66} = \alpha^2 \frac{(1-\nu)}{2} c_{11}.$$

RESULTS

Table 1. β_M at load point $k = 0{\cdot}4$ at full interaction for various d/D

$\frac{c_{22}}{c_{11}}$	$\frac{d}{D}$ \ $\frac{b}{a}$	0·2	0·4	0·6	0·8	1·0
1	$\frac{7}{8}$	0·318	0·171	0·115	0·086	0·069
	$\frac{1}{2}$	0·229	0·126	0·086	0·065	0·052
	$\frac{1}{8}$	0·067	0·042	0·030	0·023	0·019
1·5	$\frac{7}{8}$	0·296	0·156	0·104	0·079	0·063
	$\frac{1}{2}$	0·216	0·123	0·085	0·064	0·051
	$\frac{1}{8}$	0·063	0·039	0·027	0·021	0·017

Table 2. β_M at middle support section for load at $k=0{\cdot}4$ at full interaction for various d/D

$\frac{c_{22}}{c_{11}}$	$\frac{d}{D}$ \ $\frac{b}{a}$	0·2	0·4	0·6	0·8	1·0
1	$\frac{7}{8}$	0·313	0·169	0·113	0·085	0·068
	$\frac{1}{2}$	0·262	0·146	0·100	0·076	0·061
	$\frac{1}{8}$	0·110	0·082	0·061	0·047	0·038
1·5	$\frac{7}{8}$	0·292	0·154	0·103	0·078	0·062
	$\frac{1}{2}$	0·245	0·134	0·091	0·068	0·055
	$\frac{1}{8}$	0·102	0·073	0·053	0·041	0·033

Table 3. β_M at load points for various load positions, side ratios and $\frac{c_{22}}{c_{11}}$ at complete interaction

$\frac{c_{22}}{c_{11}}$	Load position k \ $\frac{b}{a}$	0·2	0·4	0·6	0·8	1·0
1·0	0·2	0·233	0·124	0·084	0·063	0·051
	0·4	0·264	0·140	0·094	0·071	0·057
	0·6	0·197	0·102	0·068	0·051	0·041
	0·8	0·013	0·005	0·003	0·002	0·002
1·5	0·2	0·225	0·118	0·080	0·060	0·048
	0·4	0·255	0·133	0·089	0·067	0·054
	0·6	0·190	0·097	0·064	0·048	0·039
	0·8	0·011	0·004	0·002	0·002	0·001

Table 4. β_M at middle support section for various load positions, side ratios and $\frac{c_{22}}{c_{11}}$ at complete interaction

$\frac{c_{22}}{c_{11}}$	Load position k \ $\frac{b}{a}$	0·2	0·4	0·6	0·8	1·0
1·0	0·2	0·232	0·123	0·082	0·062	0·050
	0·4	0·228	0·119	0·080	0·060	0·048
	0·6	0·204	0·105	0·070	0·053	0·042
	0·8	0·151	0·077	0·051	0·038	0·031
1·5	0·2	0·222	0·115	0·077	0·058	0·047
	0·4	0·218	0·112	0·075	0·056	0·045
	0·6	0·196	0·100	0·066	0·050	0·040
	0·8	0·146	0·073	0·049	0·037	0·029

DISCUSSION AND CONCLUDING REMARKS

The analysis has demonstrated qualitatively the influence of partial interaction on shear lag in continuous non-prismatic beam concrete deck systems.

The effect of shear connection on deflexion characteristics, Fig. 3, is very marked, exhibiting, as would be expected from a physical conjecture, a reduction in deflexion with increasing shear connection modulus. Deflexion curves at no interaction and at full interaction give the extreme cases. A similar phenomenon exists with the slip characteristics which exhibit negative values in parts of the span. The results in respect of slip show that negative slips can in fact occur in composite beams with supports juxtaposed as in the present problem, and most probably in continuous beams with other configurations of supports and profiles.

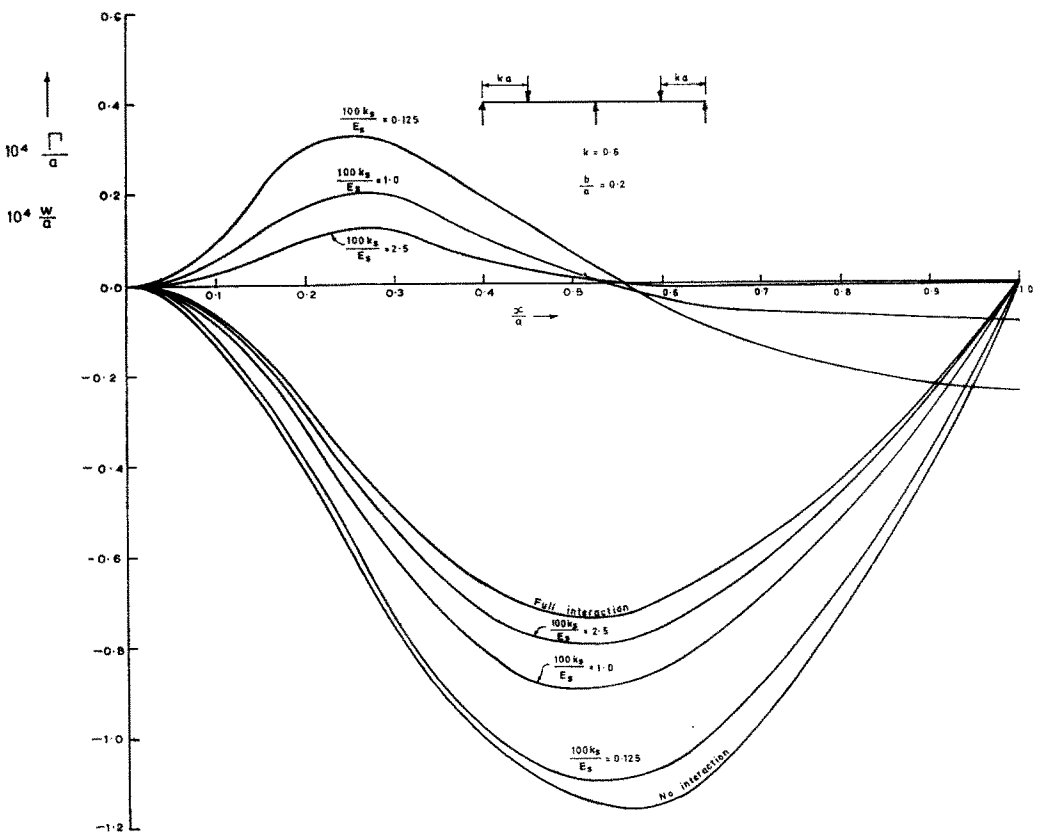

Fig. 3. Deflexion and slip characteristics for various shear connection modulus for load point $k = 0{\cdot}6$ and aspect ratio of 0·2.

Figure 4 further demonstrates the stiffening effect of the concrete plate on the steel beams through the variation of shear connection modulus with the ratio of deflexion of the interacting elements to that of the steel beam above. Figures 5(a and b) show, respectively, effective width factors obtained at the loaded point and at the middle support section as they vary with both aspect ratio, $\frac{b}{a}$, and the shear connection modulus k_s. These effective

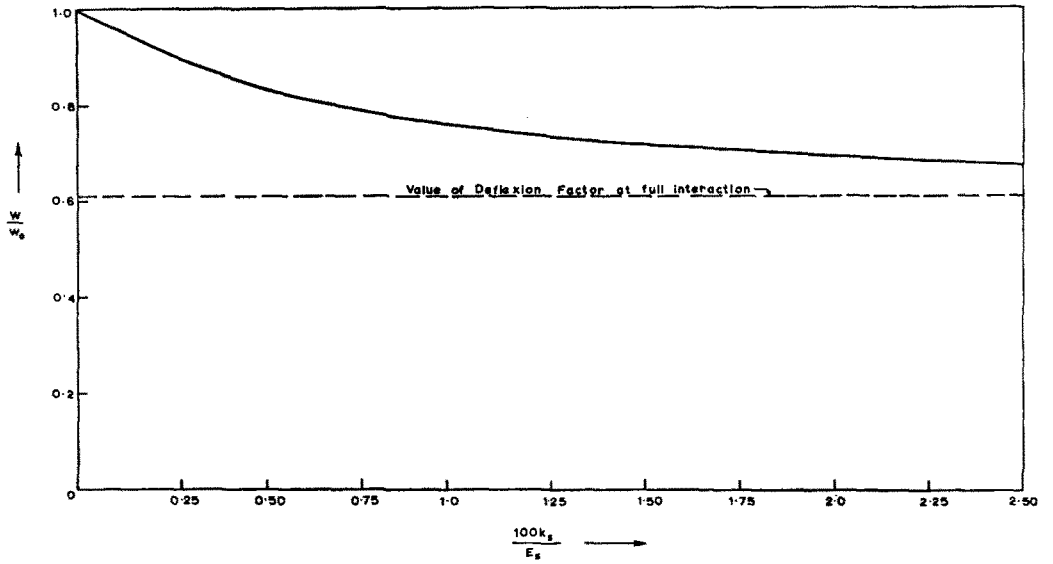

Fig. 4. The influence of shear connection modulus on deflexion of composite assembly.

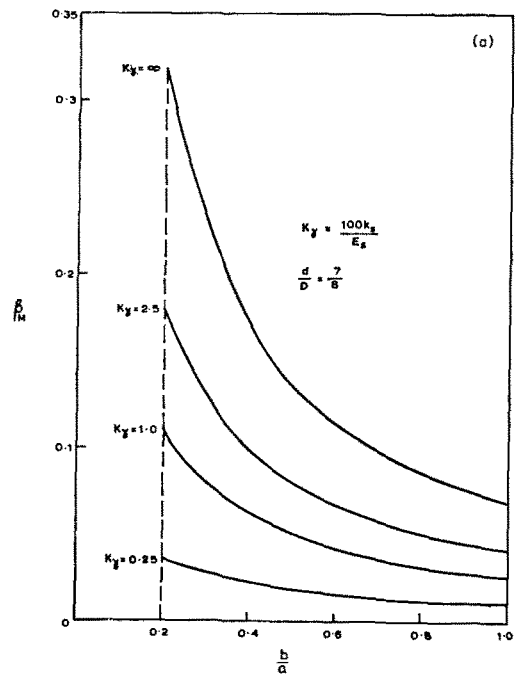

Fig. 5(a). Variation of effective width (at loaded point) with aspect ratio and shear connection modulus.

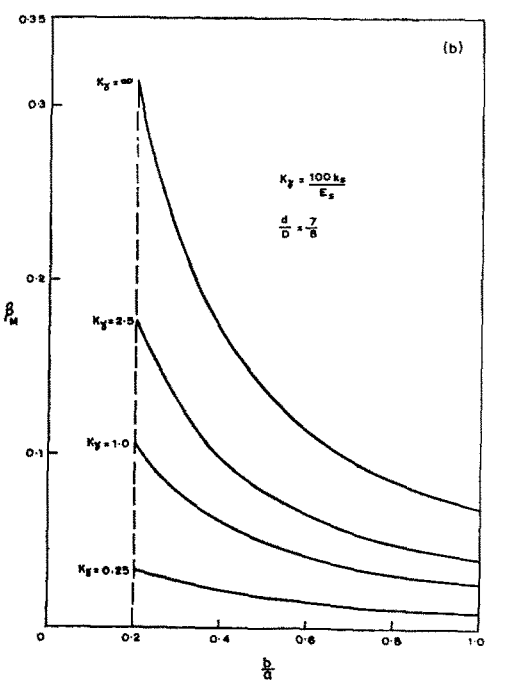

Fig. 5(b). Variation of effective width at middle reaction section with aspect ratio and shear connection modulus.

width factors, deduced from the comparison of the moment-curvature relation of the composite assembly to that of the steel beam alone, taking moment as an invariant at corresponding appropriate points, exhibit little difference between support values and the values at the loaded point. This is also noticeable for all other load positions except when the loads are $0{\cdot}8a$ from extreme supports, where effective width values under the loads vary hapazardly, although the values at the support section still exhibit the general trend of Figs. 5(b). It is thought that at this point the load is very close to the point of contraflexure of the composite assembly and consequently bending moment values are very small or close to zero giving rise to unrealistic values of effective width factors.

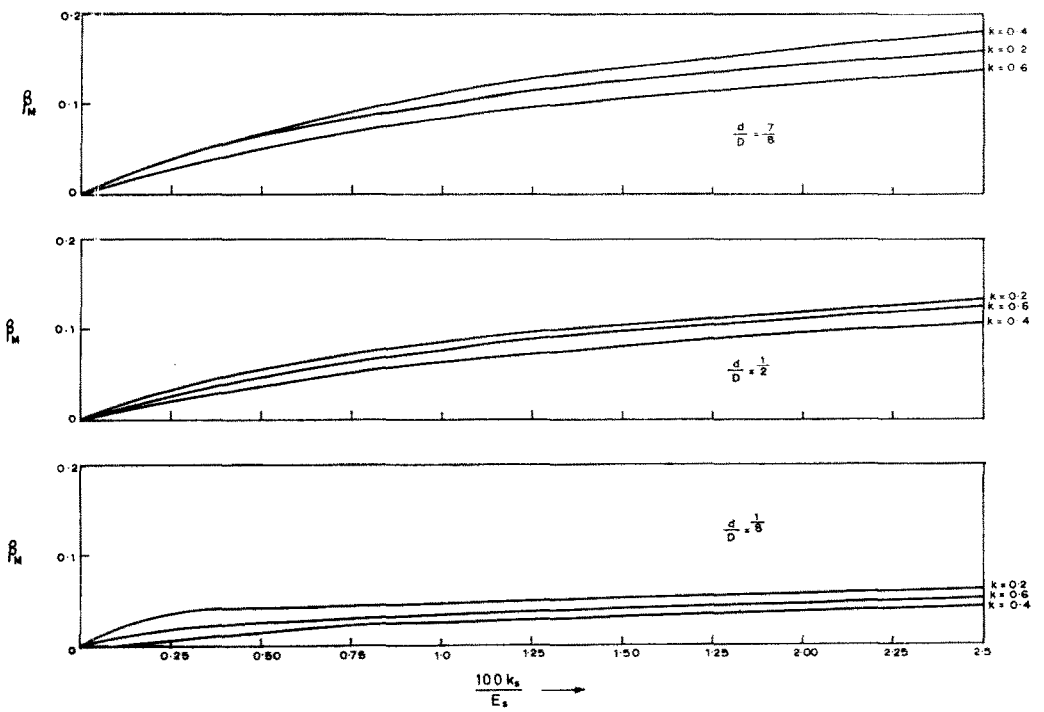

Fig. 6. Variation of effective width with shear connection modulus for different load positions and severity of variation of flexural rigidity.

Figure 6 demonstrates the influence of the severity of variation of the profile, with the middle support cross-section as in Fig. 2 for all profiles considered, on effective width factors at various k_s. It is clearly demonstrated that this severity has a marked influence on β_M. While the general trend of β_M with k_s remains similar, the values of β_M become reduced as $\frac{d}{D}$ decreases. Although between $\frac{d}{D} = \frac{7}{8}$ and $\frac{d}{D} = \frac{1}{2}$ the relative magnitudes, at least qualitatively, of effective width factors for load positions $k = 0{\cdot}2$, $k = 0{\cdot}4$ and $k = 0{\cdot}6$ remain consistent, however at $\frac{d}{D} = \frac{1}{8}$ there occurs a complete inter-change of relative magnitudes which cannot as yet be explained.

Tables 1 and 2 give respectively effective width factors at the loaded point and at the middle support section for various ratios of $\frac{d}{D}$ for the case of complete isotropy, i.e. $\frac{c_{22}}{c_{11}} = 1$ and for the case $\frac{c_{22}}{c_{11}} = 1{\cdot}5$ at full interaction.

Tables 3 and 4 on the other hand give respectively full interaction effective width factors at the loaded point and at the middle support section for various positions of applied point loads for the case of complete isotropy as well as $\frac{c_{22}}{c_{11}} = 1{\cdot}5$.

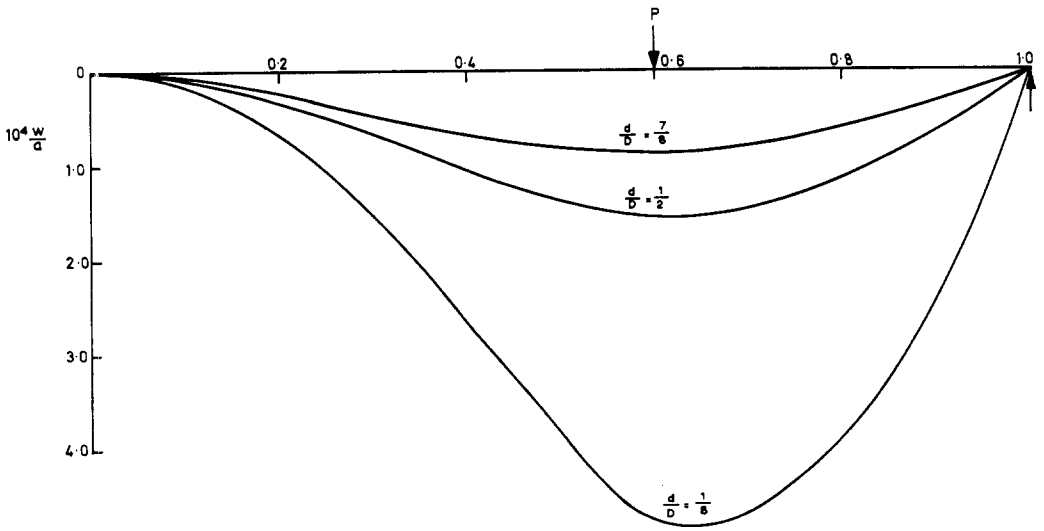

Fig. 7. Deflexion characteristics for different severity of variation of flexural rigidity.

Finally, Fig. 7 illustrates the effect of severity of variation of beam depth on deflexion. It is deducible from this curve that $\frac{d}{D} < \frac{1}{2}$ will always result in excessive transverse deflexions and should therefore be avoided in design.

Acknowledgements—The author is indebted to the University for making funds available for the computation. The author wishes to place on record his deep appreciation to the following persons: Mr. Agbalajobi and Mr. Gordon both of the Institute of Computer Sciences, University of Lagos, for helping in debugging a complex programme. In this connection thanks are also due to Dr. J. O. Sonuga; and to another colleague, Dr. K. Aderogba, for his assistance in the mathematical aspects of the paper.

REFERENCES

1. W. Metzer, *Die mittragende Breite*. Luftfahrforschung (1929).
2. E. Chwalla, Die Formeln zur Berechung der voll mittragende Breite, düner Gurt-und Rippenplatten, *Der Stahlbau* **2**, 73 (1936).
3. von K. Marguerre, Uber die Beanspruchung von Platten-tragem, *Der Stahlbau* **8**, 129 (1952).
4. A. O. Adekola, Effective widths of composite beams of steel and concrete. *Struct. Engr.* **46**, 285 (1968).

5. C. P. Siess, I. M. Viest and N. M. Newmark, Studies of slab and beam highway bridges, Part III–Small scale tests of shear connectors and composite T-beams, *Bull. Ill. Univ. Engng. Exp. Stn.* No. 396 (1952).
6. A. O. Adekola, Partial interaction between elastically connected elements of a composite beam. *Int. J. Solids Struct.* **4**, 1125 (1968).
7. A. O. Adekola, The dependence of shear lag on partial interaction in composite beams. *Int. J. Solids Struct.* **10**, 389 (1974).
8. S. Timoshenko and S. Woinowsky-Krieger, *Theory of Plates and Shells*. McGraw-Hill (1959).
9. I. S. Gradshteyn and I. M. Ryzhik, *Tables of integrals, Series and Products*. Academic Press, New York (1965).
10. I. S. Sokolnikoff, *Mathematical Theory of Elasticity*, 2nd edition. McGraw-Hill, New York (1956).

Резюме — На основании линеаризованных теорий изгиба и растяжения тонких пластин, представляют анализ взаимодействия между непризматическими балками и ортотропической бетонной плитой. Нашли, что показательное представление профилей стальных балок представляет подходящий базис для изучения молекулярного взаимодействия в непрерывных непризматических балках, и для расчета с целью проектирования подходящей и эффективной ширины плаской плиты. Изучается влияние «эластичного» модуля упругости соединения и эффект изменяющейся жесткости по отношению к изгибу стальных балок. Зависимость взаимодействия от модуля упругости в непрерывных балках демонстрируется характеристиками жесткости по отношению к изгибу и пластическому сдвигу, и также демонстрируется зависимость от степени жесткости по отношению к изгибу. Решение сводится к ограниченному случаю призматических стальных балок, к плоской бетонной плите и также к прямоугольным плитам с определенным состоянием краев.